Title:

Sensory gating precedes motor command in evolution of the corticospinal tract

Authors:

Yunuen Moreno-Lopez*, Charlotte Bichara*, Philippe Isope, Matilde Cordero-Erausquin

*These authors contributed equally to this work

Affiliation (+ present addresses):

Institut des Neurosciences Cellulaires et Intégratives, CNRS UPR 3212, Université de Strasbourg, Strasbourg, France

M.C.E. : https://orcid.org/0000-0002-1623-1773

P.I.: https://orcid.org/0000-0002-0630-5935

Y.M.L.'s present address: Burke Neurological Institute, White Plains, New York, NY 10605, United States

Throughout mammals evolution, the contribution of the corticospinal tract (CST) to motor control progressively increases, culminating in primates with tight control of skilled movements such as independent finger dexterity[1]. Although cortico-motoneuronal connections have been shown to be absent or very rare in rodents[2-5], it is generally assumed by analogy with primates that the main function of the CST is to convey motor commands. Yet the CST has been shown to have other functions[1], such as sensory gating. By differentially filtering out sensory signals at their entry point in the spinal cord[6,7], sensory gating is thought to have evolved to increase the gain of relevant feedback information during voluntary movement to improve execution of skilled movements[8-10]. Here we show that, unexpectedly, sensory gating is the essential function of the lumbar CST in mice while lumbar motor command mainly involves non-CST pathways. By sequentially investigating each stage of the corticofugal pathways for motor command and sensory gating, we found that they both originate in the same cortical area but follow segregated paths. The hindlimb motor command is mainly relayed through subcortical supraspinal motor centers, and is only anecdotally encoded by the CST, requiring a propiospinal relay in the upper cord. In contrast, corticospinal neurons are essential for sensory gating, and act directly through a population of lumbar interneurons. Our results reveal that the original function of the CST in mammals, still prominent in rodents, is sensory gating, not motor control. This pathway appears to have been later selected through evolution to serve other functions, such as refined motor commands, eventually yielding direct CST-to-motoneuron connection in primates. The rodent lumbar CST thus serves as a prototypical paradigm to study, in isolation, the primary role of CST in sensory gating.

The rodent sensorimotor cortex has a highly somatotopic organization[11]. Mainly studied in a motor command perspective, it has been repeatedly mapped for its ability to provoke motor contraction[11,12], but never yet with regard to its ability to induce sensory gating. This cortically-evoked inhibition of sensory information transfer between primary afferents and the central nervous

system is mediated by presynaptic depolarization of the central terminals of primary afferents[13] and can be experimentally assessed by recording cortically-evoked dorsal root potentials (DRPs, Fig. 1A). We thus recorded DRPs *in vivo* in lumbar roots L4-L6 (conveying hindlimb sensory inputs) of Thy1::ChR2 mice, expressing channelrhodopsin2 in layer V cortical neurons[14], and mapped the cortical area eliciting DRPs and muscle contractions in the hindlimb (Fig. 1A,B). Using photostimulations at the surface of the cortex, we identified the area inducing the largest DRPs (center: AP=-0.75 mm, L=1.5 mm; Fig. 1C, n=7 mice) and the largest electromyographic (EMG) signal in the tibialis anterior (center: AP=-0.75 mm, L=1.75mm, n=5 mice; Fig. 1C), demonstrating for the first time in rodents that they overlap. These latter results were consistent with previous functional mapping of the motor cortex in mice[11,12] although this area is labelled as primary sensory cortex in some atlases and studies [15-17]; we thus use the conservative term “sensorimotor cortex”. Our results show that sensory gating and motor commands originate from the same area of the cortex.

We next investigated the spinal circuit underlying cortically-evoked DRPs. DRPs can also be segmentally-evoked, by the activation of a neighboring root; this dampens sensory inputs through GABA-dependent primary-afferent depolarization[13] although cholinergic pathways have also been described[18]. In addition, it has recently been shown that GABAergic terminals presynaptic to proprioceptive fibers arise from GAD65 interneurons[19,20]. We thus investigated whether the CST directly targets GAD65-expressing spinal lumbar neurons that could in turn inhibit primary afferents. In TdTomato-flex mice crossed with GAD65::GFP mice, we infected cortical neurons located in the area inducing hindlimb DRPs and EMG (Extended data Fig.1) with a viral monosynaptic anterograde transynaptic tool (AAV1-CBA::WGA-Cre) encoding the Cre-recombinase fused to the wheat germ agglutinin (WGA). The fusion with WGA provides transynaptic properties to Cre, which is then transferred to cortical monosynaptic targets where it unlocks the expression of TdTomato (see Methods, Extended data Fig. 2). We evaluated the proportion of GAD65+ neurons among corticospinal post-synaptic neurons (CSPNs) revealed by Td-Tomato expression (Fig. 1D-E): 16.4±3.2% of CSPNs were GAD65::GFP+ (n=3 mice), suggesting that the cortically-evoked DRP could be

mediated by the activation of GAD65 CSPNs within a circuit involving a single spinal player. By performing a similar experiment in ChAT::EGFP mice, only 2.2±1.8% of CSPNs were ChAT::EGFP positive (n=4 mice), excluding a direct contribution of a cholinergic mechanism (extended data Fig. 3).

Although sensory gating signals and motor commands originate from the same area in the mouse sensorimotor cortex, they may not share the same corticofugal pathway and spinal circuits. We thus interrogated the contribution of indirect cortical-to-spinal pathways to these two functions (Fig. 2). As broad photostimulation of the cerebral cortex in Thy1::ChR2 activates a variety of cortical neurons[14]; we selectively lesioned the direct CST (Fig. 2B) using an electrolytic lesion at the level of the pyramidal decussation (pyramidotomy). This protocol spares potential CST collaterals targeting the red nucleus or the reticular nucleus branching more rostraly[21,22] as well as rubrospinal or reticulospinal tracts that can be activated by corticorubral or corticoreticular neurons (Fig. 2B). Cortically-evoked DRPs were completely abolished by this pyramidotomy (DRP amplitude 3.8 μV± 0.32μV before, 0.30 μV± 0.12μV after, n=3 mice, p=0.006), whereas cortically-evoked EMGs were hardly affected (S/N Ratio 3.3± 0.61 before, 2.2 ± 0.1 after, n=4 mice, p=0.517, all Z-Scores above significance after lesion, Extended Data table 1B) (Fig. 2C-D). This demonstrates that indirect cortical-to-spinal pathways (involving supraspinal motor centers) do not encode cortically-evoked DRPs but have a prominent role for cortically-evoked motor contraction of the hindlimb. Our results show that, in rodents, the lumbar CST mediates cortically-evoked DRPs and thus sensory gain at the primary afferent level.

Although the contribution of the rubrospinal or reticulospinal tracts to motor command is well acknowledged in both rodents and primates, the CST is also believed to encode motor drive[7]. This could have been underrated by simultaneous stimulation of the indirect cortical-to-spinal pathways in Thy1::ChR2 mice. We thus directly interrogated the contribution of the CST to motor contraction by targeting exclusively these neurons through injection of a ChR2-encoding retrograde AAV in the

92 lumbar spinal cord (Fig. 3A). The infected corticospinal neurons were found in the area delimited by
93 the functional mapping of hindlimb muscle contraction and DRP (Fig. 3B-C). Their photostimulation
94 (at the cortical level) induced a robust EMG signal (S/N Ratio 1.65±0.14, n=4 mice, Fig. 3E, upper),
95 demonstrating that CS neurons had indeed the ability to encode motor contraction. Because some CS
96 neurons are known to send collaterals to supraspinal regions involved in motor command[22], we next
97 addressed whether the recorded motor command traveled through the direct cortical-to-spinal
98 branch of CS neurons or via supraspinal relays. A caudal pyramidotomy completely abolished the
99 EMG signal evoked by cortically activating CS neurons (S/N Ratio 0.9±0.12; n=3 mice, p=0.013; all Z
100 scores below significance after pyramidotomy, extended Data table 1C) (Fig. 3D-E). This
101 demonstrates that, even if CST may have supraspinal collaterals, these do not encode motor output.
102 Rather, it is through their direct spinal branch that CS neurons are able to drive motor command,
103 although their contribution appears minor when other cortical neurons are simultaneously activated.

104

105 Because both the sensory gating and motor command of a given limb are encoded by the same
106 sensorimotor cortical area and can be relayed by the same direct corticospinal tract, we next
107 interrogated how these functions are segregated at the spinal level. It is documented that CS
108 neurons projecting to the lumbar spinal cord can have collaterals at the cervico-thoracic level[23].
109 There, they can contact cervical propriospinal neurons (including Chx10-expressing ones[24,25]) that in
110 turn project to lumbar motoneurons and can be involved in motor command[24]. In order to test
111 specifically the contribution of the lumbar branch of CS neurons, without risking antidromic
112 stimulation of rostral collaterals, we combined the transynaptic tool presented above with an
113 intersectional approach at the lumbar level. We first identified the lumbar area containing CSPNs
114 neurons, after cortical injection of AAV1-CBA::WGA-Cre in TdTomato-flex mice (Fig. 4A): CSPNs were
115 concentrated in spinal lumbar segments L2-L3, rostral to the large pools of motoneurons, in the
116 contralateral deep dorsal horn (laminae IV to VII) (Fig. 4B). They were mostly located in the medial

zone, lateral to the dorsal funiculus, where the CST fibers penetrate the grey matter. We thus combined the cortical injection of AAV1-CBA::WGA-Cre with the injection of an AAV encoding for a Cre-dependent form of ChETA (a ChR2 variant[26]) in the lumbar segment L3, in the medial third of the dorsal horn (Fig. 4C). In this way, we restricted the expression of ChETA to the lumbar CSPNs (Fig. 4C, D). Photostimulation of these lumbar CSPN through the spinal surface induced DRPs in the ipsilateral lumbar root (3.58 ± 0.67 µV, n=5 mice, Fig. 4E-G), demonstrating that hindlimb sensory gating at the primary afferent level is directly controlled by the CST projecting to the lumbar cord. However, photoactivation of these same lumbar CSPNs did not elicit any muscle contraction as attested by flat EMG recordings (S/N Ratio 0.9±0.01; n=4 mice, Z-Scores below significance, extended Data table 1D) (Fig. 4E-G), suggesting that CST-evoked motor command is mediated by a spinal circuit located at another spinal level. Cortically-evoked DRPs and EMGs thus follow a similar corticofugal pathway that then segregates at the spinal level.

Altogether, our results demonstrate a segregation of pathways involved in cortically-evoked sensory gating vs. motor control. The direct corticospinal tract in isolation (downstream its supraspinal collaterals) is able to induce motor contraction through spinal targets possibly located at the cervico-thoracic level as recently suggested[17]. There, they could relay the command to propriospinal neurons some of which are known to be premotor[24]. However, we show that motor command mainly involves non-CST pathways, most likely cortico-rubral, or -reticular ones. On the other hand, the major and essential role of the lumbar rodent CST appears to be hindlimb sensory gain at the primary afferent level, through a population of lumbar CSPN whose activation is sufficient to produce DRPs. This should not minor the importance of the CST in coordinated locomotion and skilled movements, as appropriate modulation of sensory feedback at the spinal cord level is essential for these functions[27,28]. While the CST has long been known to have different functions and to have progressively evolved towards an essentially fine motor tract[1], we here show that its prominent role in the rodent lumbar cord is sensory gating. This suggests that sensory gating by the CST has not evolved secondary to motor control, but rather precedes motor control in the evolution of the CST.

143 This paradigm shift also forces re-interpretation of previous studies aiming at promoting CST function
144 in a therapeutical perspective, whether in mouse models of spinal injury or neurodegenerative
145 diseases such as amyotrophic lateral sclerosis. While most of these studies have exclusively
146 considered motor command aspects, our results provide a new perspective to analyze these efforts
147 by taking into account the primary role of rodent lumbar CST, i.e. sensory gating**.**

148 **Main references:**

149 1 Lemon, R. N. Descending pathways in motor control. Annu Rev Neurosci 31, 195-218 (2008).

150 2 Alstermark, B. & Ogawa, J. In vivo recordings of bulbospinal excitation in adult mouse
151 forelimb motoneurons. J Neurophysiol 92, 1958-1962 (2004).

152 3 Alstermark, B., Ogawa, J. & Isa, T. Lack of monosynaptic corticomotoneuronal EPSPs in rats:
153 disynaptic EPSPs mediated via reticulospinal neurons and polysynaptic EPSPs via segmental
154 interneurons. J Neurophysiol 91, 1832-1839 (2004).

155 4 Gu, Z. et al. Control of species-dependent cortico-motoneuronal connections underlying
156 manual dexterity. Science 357, 400-404 (2017).

157 5 Weidner, N., Ner, A., Salimi, N. & Tuszynski, M. H. Spontaneous corticospinal axonal plasticity
158 and functional recovery after adult central nervous system injury. Proc Natl Acad Sci U S A 98, 3513-
159 3518 (2001).

160 6 Moreno-Lopez, Y., Olivares-Moreno, R., Cordero-Erausquin, M. & Rojas-Piloni, G.
161 Sensorimotor Integration by Corticospinal System. Front Neuroanat 10, 24,
162 doi:10.3389/fnana.2016.00024 (2016).

163 7 Ueno, M. et al. Corticospinal Circuits from the Sensory and Motor Cortices Differentially
164 Regulate Skilled Movements through Distinct Spinal Interneurons. Cell Rep 23, 1286-1300 e1287,
165 doi:S2211-1247(18)30525-4 [pii] (2018).

166 8 Ebbesen, C. L. & Brecht, M. Motor cortex - to act or not to act? Nat Rev Neurosci 18, 694-705,
167 (2017).

168 9 Confais, J., Kim, G., Tomatsu, S., Takei, T. & Seki, K. Nerve-Specific Input Modulation to Spinal
169 Neurons during a Motor Task in the Monkey. J Neurosci 37, 2612-2626 (2017).

170 10 Seki, K., Perlmutter, S. I. & Fetz, E. E. Sensory input to primate spinal cord is presynaptically
171 inhibited during voluntary movement. Nat Neurosci 6, 1309-1316 (2003).

172 11 Ayling, O. G., Harrison, T. C., Boyd, J. D., Goroshkov, A. & Murphy, T. H. Automated light-
173 based mapping of motor cortex by photoactivation of channelrhodopsin-2 transgenic mice. Nat
174 Methods 6, 219-224 (2009).

175 12 Li, C. X. & Waters, R. S. Organization of the mouse motor cortex studied by retrograde tracing
176 and intracortical microstimulation (ICMS) mapping. Can J Neurol Sci 18, 28-38 (1991).

177 13 Rudomin, P. & Schmidt, R. F. Presynaptic inhibition in the vertebrate spinal cord revisited.
178 Exp Brain Res 129, 1-37 (1999).

179 14 Arenkiel, B. R. et al. In vivo light-induced activation of neural circuitry in transgenic mice
180 expressing channelrhodopsin-2. Neuron 54, 205-218 (2007).

181 15 Kirkcaldie, M., Watson, c., Paxinos, G. & Franklin, K. in Australian Neuroscience Society
182 Annual Conference.

183 16 Liu, Y. et al. Touch and tactile neuropathic pain sensitivity are set by corticospinal projections.
184 Nature 561, 547-550 (2018).

185 17 Karadimas, S. K. et al. Sensory cortical control of movement. Nat Neurosci,
186 doi:10.1038/s41593-019-0536-7 (2019).

187 18 Hochman, S., Shreckengost, J., Kimura, H. & Quevedo, J. Presynaptic inhibition of primary
188 afferents by depolarization: observations supporting nontraditional mechanisms. Ann N Y Acad Sci
189 1198, 140-152 (2010).

190 19 Betley, J. N. et al. Stringent specificity in the construction of a GABAergic presynaptic
191 inhibitory circuit. Cell 139, 161-174 (2009).

192 20 Hughes, D. I. et al. P boutons in lamina IX of the rodent spinal cord express high levels of
193 glutamic acid decarboxylase-65 and originate from cells in deep medial dorsal horn. Proc Natl Acad
194 Sci U S A 102, 9038-9043 (2005).

195 21 Alstermark, B. & Pettersson, L. G. Skilled reaching and grasping in the rat: lacking effect of
196 corticospinal lesion. Front Neurol 5, 103, doi:10.3389/fneur.2014.00103 (2014).

197 22 Akintunde, A. & Buxton, D. F. Origins and collateralization of corticospinal, corticopontine,
198 corticorubral and corticostriatal tracts: a multiple retrograde fluorescent tracing study. Brain Res 586,
199 208-218 (1992).

200 23 Kamiyama, T. et al. Corticospinal tract development and spinal cord innervation differ
201 between cervical and lumbar targets. J Neurosci 35, 1181-1191 (2015).

202 24 Ni, Y. et al. Characterization of long descending premotor propriospinal neurons in the spinal
203 cord. J Neurosci 34, 9404-9417 (2014).

204 25 Ueno, M., Hayano, Y., Nakagawa, H. & Yamashita, T. Intraspinal rewiring of the corticospinal
205 tract requires target-derived brain-derived neurotrophic factor and compensates lost function after
206 brain injury. Brain 135, 1253-1267 (2012).

207 26 Gunaydin, L. A. et al. Ultrafast optogenetic control. Nat Neurosci 13, 387-392 (2010).

27 Akay, T., Tourtellotte, W. G., Arber, S. & Jessell, T. M. Degradation of mouse locomotor pattern in the absence of proprioceptive sensory feedback. Proc Natl Acad Sci U S A 111, 16877-16882 (2014).

28 Fink, A. J. et al. Presynaptic inhibition of spinal sensory feedback ensures smooth movement. Nature 509, 43-48 [pii]

Methods:

Animal models. This study was carried out in strict accordance with the national and international laws for laboratory animal welfare and experimentation and was approved in advance by the Ethics Committee of Strasbourg (CREMEAS; CEEA35; agreement number/reference protocol: APAFIS# 12982 - 2017122217349941 v3). The following mice strains were used (adult males and females): Thy1::ChR2 (Cg-Tg(Thy1-COP4/EYFP)18Gfng/J, Jackson Laboratory), TdTomato-Flex (*Gt(ROSA)26Sor*$^{tm14(CAG\text{-}tdTomato)Hze}$/J, Jackson Laboratory), ChAT::EGFP[29], GAD65::GFP[30]. All lines except GAD65::GFP were back-crossed (at least 10 generations) on a CD1 background. GAD65::GFP were on a C57Bl6/J background. The mice were housed in the Chronobiotron facility (UMS3415, CNRS, University of Strasbourg) in accordance with the European convention 2010/63/EU on the protection of animals used for scientific purposes.

Electrophysiological recordings.

EMG recording: Ketamine/Xylazine anesthesia was chosen to minimally affect muscular tone. After the initial anesthesia (150 mg/kg of ketamine, Imalgene 1000 and 10 mg/kg of Xylazine, Rompun 20%), complementary doses of Ketamine were given when the animal was showing signs of awakening (additional doses bridged by short exposure to Isoflurane 1–1.5%)[31]. Concentric EMG needle electrodes (Myoline Xp) were inserted in the *tibialis anterior* muscle of the animals and a ground electrode was inserted in the tail. Responses were collected with a recording amplifier (IR183A, Cygnus technology) in series with a second amplifier (Brownlee Precision, model440). The traces were filtered with a bandwidth of 0.1 Hz–10 kHz, recorded with Spike 2 software (version 8.00, CED, Cambridge, UK), and analyzed off line with Clampfit (pCLAMP, version 10.7) and home-made python routines (WinPython 2.7.10, Python Software Fundation) . EMG responses were recorded after cortical or spinal photostimulation (see below), and the response to 3 consecutive stimulations was averaged for analysis. The area under the curve of the rectified average trace was calculated in a window of 30ms, either 40 ms before (baseline noise, N) or 10 ms after (signal, S) the onset of the stimulation. The EMG response

was presented as the S/N ratio. In CST lesion experiments, all S/N ratios were expressed as a % of the control S/N (average of 3 responses before the lesion). The noise level (S/N of 1) was similarly expressed as a % of the above defined control S/N.

DRP recording: Under isofluorane (1.5-2%) anesthesia, the mice spinal cord was fixed with the spinal cord unit of a stereotaxic frame (Narishige instruments). A laminectomy was performed to expose the surface of lumbar L3-L6 spinal cord segments. A dorsal root (L4-L6) was dissected, cut before the DRG, and suctioned with a glass pipet. An agar pool was created on the exposed spinal cord, and filled with NaCl 0.9%. The amplifiers/filters/software used were the same as for the EMG recordings. DRPs in response to 30 successive cortical or spinal photostimulations (see below) were averaged for analysis. The amplitude of the response from the onset to the peak was measured using Clampfit 10.0. The amplitude of the noise was similarly measured during sweeps without photostimulation.

Cortical photostimulation. Optogenetic stimulation of the cortex was performed on anesthetized animals while recording EMG or DRP. For the cortex, a craniotomy of approximately 9mm^2 was performed under stereo microscope on the contralateral side from the recording site. Muscle contraction, measured by EMG, was evoked by photostimulation with a 250 µm-probe (473 nm laser source PSU-III-FDA) using the following protocol: trains of 6 pulses, 1 ms duration, 2 ms interval; 15 s minimum between each train. DRPs were elicited by photostimulation with a 105 µm-probe (460 nm LED source, Prizmatix) using the following protocol: trains of 5 pulses of 8 ms, 1 ms interval and 2 s between each train. In both cases, the probe was moved at the surface of the cortex along a 500 µm-spaced grid. Isopotential contour plots were created, using for EMGs the S/N and for DRPs the peak amplitude (both normalized to the largest values in each animal) at each photostimulation point in the cortex, using a linear interpolation on a set of X, Y, Z triples of a matrix. For EMG, only S/N ratio above significance (Z-Score>3, Extended Data table 1A) were considered for the analysis. Then the isopotentials contours were superimposed on the metric planes of the top view of the cortex[15].

Spinal cord photostimulation. Optogenetic stimulation of the spinal cord was performed on anesthetized mice after laminectomy (described above for DRPs recordings), using a 1 mm probe (LED

source) placed on the surface of the lumbar spinal cord (on top of the injection site). The stimulation trains were those used for cortical stimulation. EMG and DRP recordings were sequentially performed and required to alternate between different types of anesthesia: isoflurane (craniotomy and laminectomy surgery), ketamine/xylazine (EMG recording), isoflurane 1.5–2 % (DRPs recordings).

Pyramidotomy. Electrolytic lesion of the CST was performed in a subset of THY1::ChR2 and ChR2 retrogradely labeled mice, with 200 ms pulses, 30 mA using a constant current stimulator (Digitimer Ltd thorug) through a silver bipolar electrode inserted in the pyramidal decussation (3.5-4 mm caudal to Bregma, 6 mm deep). The brain was removed for histological analysis at the end of the experiment.

Cortical and spinal injections.

Brain injections (1.5–2 mm lateral, 0.5–1 mm caudal to Bregma, 0.5 mm deep) were performed as previously described[32] under isoflurane anesthesia (2–3%). Briefly, 90 to 270 nL of virus was injected by manual pressure using a 5 mL syringe coupled to a calibrated glass capillary, under visual control. Spinal injections were performed using a similar manual pressure protocol. The pipette was inserted in the exposed space between two vertebrae (T13-L1, corresponding to spinal L4), as previously described[33]. 0.45 µL of virus was injected 300 µm lateral to the midline and 300-400 µm deep. In both cases, Manitol 12.5% was injected i.p. (0.2 – 0.5 ml) after the surgery to enhance vector spread and improve transduction[34]

The animals were kept 2 weeks for the retroAAV injections and a minimum 5 weeks for dual injections before in vivo DRPs and/or EMGs recordings or histological analysis.

Virus. AAV2/1-CBA-WGA-CRE-WPRE was purchased at the molecular tools platform at the Centre de recherche CERVO (Québec, Canada), and was used at a titer of $8x10^{12}$ vg/ml. AAV-Ef1a-DIO ChETA-EYFP was a gift from Karl Deisseroth[26] (Addgene viral prep # 26968-AAV9; http://n2t.net/addgene:26968 ; RRID:Addgene_26968) and was used at a titer of 1×10^{13} vg/mL. AAV-CAG-hChR2-H134R-tdTomato was a gift from Karel Svoboda[35] (Addgene viral prep # 28017-AAVrg; http://n2t.net/addgene:28017 ; RRID:Addgene_28017), and was used at a titer of 7×10^{12} vg/mL.

Histology

Mice were transcardially perfused with PB followed by 4% paraformaldehyde (PFA) in PB 0.1M, or, if histological analysis followed electrophysiological recordings, the brain and spinal cord were post-fixed overnight in PFA 4% in PB 0.1M. Serial 50 µm brain (coronal or sagittal) and spinal (transverse or sagittal) sections were performed on a vibratome (Leica VT1000 S) and mounted using a DAPI staining mounting medium (Vectashield, Vector laboratories).

Image analysis. The extend of the cortical injection site was estimated by measuring the spread of reporter protein fluorescence (TdTomato) in the layer V of the cortex. The intensity of fluorescence was analyzed as previously described[36,37] on evenly spaced (250 µm apart) transverse brain sections imaged with a microscope (Axio Imager 2, Zeiss). Briefly, the "Plot Profile" function of ImageJ software (W. Rasband, National Institutes of Health) was used to measure the intensity of fluorescence along the horizontal axis of a 6000x250 µm rectangle containing the layer V of the cortex (Extended data Fig. 1). These values were normalized to the highest intensity for each animal, and used to plot a density map of each injection site. The contour of the injection area was defined as 30% of the maximal intensity, corresponding to the approximate intensity of individual neurons.

Spatial distribution of corticospinal post-synaptic neurons: Spinal_lumbar sections (50µm) were mounted serially and imaged using a Zeiss epifluorescence microscope or a Leica SP5 II confocal microscope. Images were aligned manually with Photoshop using the central canal and the dorsal funiculus as landmarks. Each labeled neuron was assigned coordinates corresponding to its distance to the center of the central canal (X and Y) and the index of the slice containing it (Z). This was used to calculate the number of labeled neurons every 100 µm x 100 µm bins (XxY) (or 200 µm x200 µm X x Z) in order to build density plots.

Quantification and statistical analysis. The mean and standard deviation of the Noise were measured from the 3 Noise values obtained from each EMG recording, and used to calculate the Z-scores. The Z-score of each EMG response to the stimulation was calculated using the following equation:

$$\text{Z-score} = \frac{\text{Signal- mean Noise}}{\text{standard deviation of Noise}}$$

A Z-score of 1.96 or 3 corresponding to a significance level of 0.05 or 0.001 was chosen to discriminate significant responses from non-significant ones. The conservative choice of threshold was chosen in agreement with visual inspection of the traces, to ensure that any EMG responses was not simply due to noise. For each tests, the normality and variance equality were verified by SigmaPlot (Version 13, Copyright © 2014 Systat Softwara, Inc) using Shapiro-Wilk and Brown-Forsythe's methods, before we applied the parametric tests. All the data were analyzed using a one-way ANOVA and a post-hoc test was performed only if an effect showed statistical significance. The P-values for multiple comparison were measured using Holm-Sidak's method. Error bars in all Figures represent mean ± s.e.m., *$P < 0.05$, NS, no statistical significance ($P \geq 0.05$). The power of the tests was systematically attested to be above the desired power of 0.80.

Methods references:

29 von Engelhardt, J., Eliava, M., Meyer, A. H., Rozov, A. & Monyer, H. Functional characterization of intrinsic cholinergic interneurons in the cortex. J.Neurosci. 27, 5633-5642 (2007).

30 Lopez-Bendito, G. et al. Preferential origin and layer destination of GAD65-GFP cortical interneurons. Cereb Cortex 14, 1122-1133 (2004).

31 Tennant, K. A. et al. The organization of the forelimb representation of the C57BL/6 mouse motor cortex as defined by intracortical microstimulation and cytoarchitecture. Cereb Cortex 21, 865-876 (2011).

32 Cetin, A., Komai, S., Eliava, M., Seeburg, P. H. & Osten, P. Stereotaxic gene delivery in the rodent brain. Nat Protoc 1, 3166-3173 (2006).

33 Tappe, A. et al. Synaptic scaffolding protein Homer1a protects against chronic inflammatory pain. Nat Med 12, 677-681 (2006).

34 Tjolsen, A., Berge, O. G., Hunskaar, S., Rosland, J. H. & Hole, K. The formalin test: an evaluation of the method. Pain 51, 5-17 (1992).

35 Mao, T. et al. Long-range neuronal circuits underlying the interaction between sensory and motor cortex. Neuron 72, 111-123 (2011).

36 Lorenzo, L. E., Ramien, M., St Louis, M., De Koninck, Y. & Ribeiro-da-Silva, A. Postnatal changes in the Rexed lamination and markers of nociceptive afferents in the superficial dorsal horn of the rat. J.Comp Neurol. 508, 592-604 (2008).

37 Mesnage, B. et al. Morphological and functional characterization of cholinergic interneurons of the dorsal horn of the mouse spinal cord. J Comp Neurol 519, 3139-3158 (2011).

Acknowledgements:

We thank the following for providing/generating specific mouse lines: Gábor Szabó for GAD65::GFP, Jakob von Engelhardt for ChAT::EGFP. YML was supported by a postdoctoral fellowhips from the Fondation pour la Recherche Médicale (SPF20160936264) and CB was funded by a fellowship from the Ministère de la Recherche. We thank Dr. Sophie Reibel-Foisset and the staff of the animal facility (Chronobiotron, UMS 3415 CNRS and Strasbourg University) for technical assistance. We also thank Yves De Koninck, Frédéric Doussau and Didier Desaintjan for critical reading of the manuscript.

Author contributions:

M.C.E. initiated the project. Y.M.L., C.B., P. I. and M.C.E. designed experiments and interpreted the data. Y.M.L. and C.B. performed the experiments. M.C.E. wrote the paper with contributions from all of the authors.

Competing interest declaration: The authors declare no competing financial interests.

Additionnal information: Correspondence and requests for materials should be addressed to M.C.E.

Life sciences reporting summary: see attached file

Corresponding author: M.C.E.

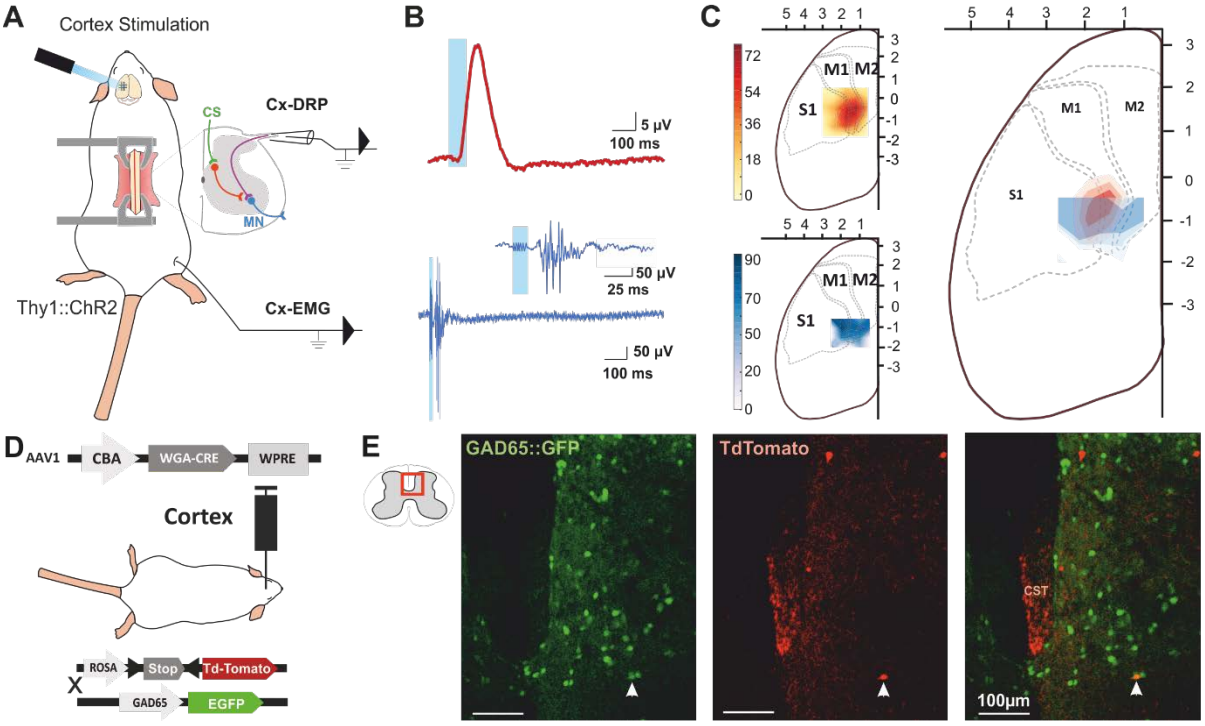

Figure 1. The same cortical area evokes dorsal root potentials and muscular contractions of the hindlimbs.

A. Schematic experimental design for cortically-evoked (Cx-) DRP and EMG recordings elicited by photostimulation of the sensorimotor cortex of Thy1::ChR2 mice. DRPs correspond to the presynaptic depolarization of primary afferents propagating antidromically to the suction recording electrode while EMGs are recorded in the *tibialis anterior* muscle.

B. Representative traces of cortically-evoked DRP (top trace, average of 30 sweeps) and EMG (bottom trace, average of 3 sweeps) after photostimulation (blue window) of the contralateral cortex.

C. *Left,* Heatmaps of the amplitude of the responses of cortically-evoked DRPs (top) and EMGs (bottom) in % or the maximum response. *Right*, Overlap of the two maps (red: DRP, blue: EMG) presented as isopotential contour plots (three color grades corresponding to 37%, 50% and 63% of maximum value). Coordinates of the cortex are expressed in mm and centered on *Bregma*. M1, M2, S1: primary motor, secondary motor, and primary sensory cortices, according to the Paxinos atlas[15].

D. Schematic experimental design to identify GAD65-expressing neurons amongst corticospinal neurons targets: AAV1-CBA-WGA-CRE was injected in the sensorimotor cortex of TdTomato-flex X GAD65::GFP mice.

E. Confocal view (z projection) of a mouse lumbar dorsal horn from the experiment presented in F (localization of the view indicated in the inset). A corticospinal postsynaptic neuron (expressing TdTomato after transynaptic transfer of WGA-Cre) also expresses GAD65::GFP. CST: corticospinal tract.

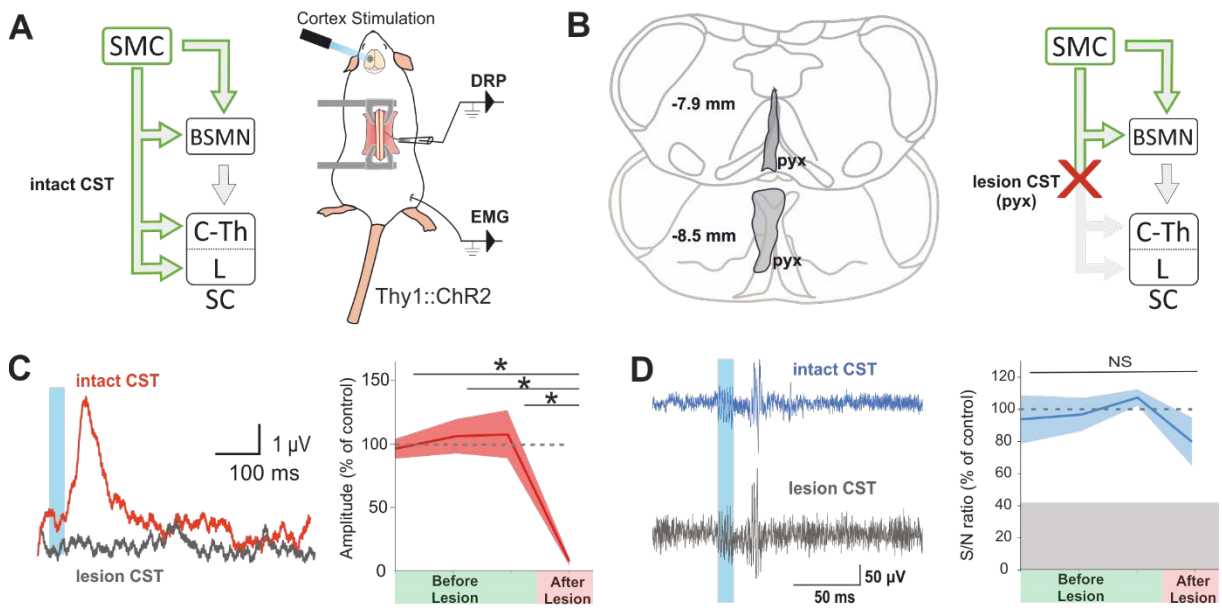

Figure 2. The corticospinal tract is essential for cortically-evoked inhibition of primary afferents.

A. *Left*, diagram showing direct and indirect cortical-to-spinal paths. In green: paths potentially activated by photostimulation in the cortex of Thy1::ChR2 mice. *Right*, recording design.
B. *Left*, extent of the pyramidal lesion (in grey, pyx) in the frontal plane (distance to *Bregma* indicated) in two animals whose recordings are respectively illustrated in C and D. *Right*, diagram showing the indirect cortical-to-spinal paths spared by the pyramidotomy.
C. *Left*, Representative traces of cortically-evoked DRP recording before (red) and after (grey) CST lesion (average of 30 traces). *Right*, the pyramidotomy abolishes cortically-evoked DRPs (p= 0.006, one-way ANOVA, n= 3 mice). Post-hoc test Holm-Sidak, *P < 0.05
D. *Left*, Representative traces of cortically-evoked EMG recording before (blue) and after (grey) pyramidal lesion (average of 3 traces). *Right*, There is no significant change in the S/N ratio of the EMG response before and after the pyramidal lesion (p=0.517, one-way ANOVA, n= 4 mice). Grey zone: noise level (see Methods).

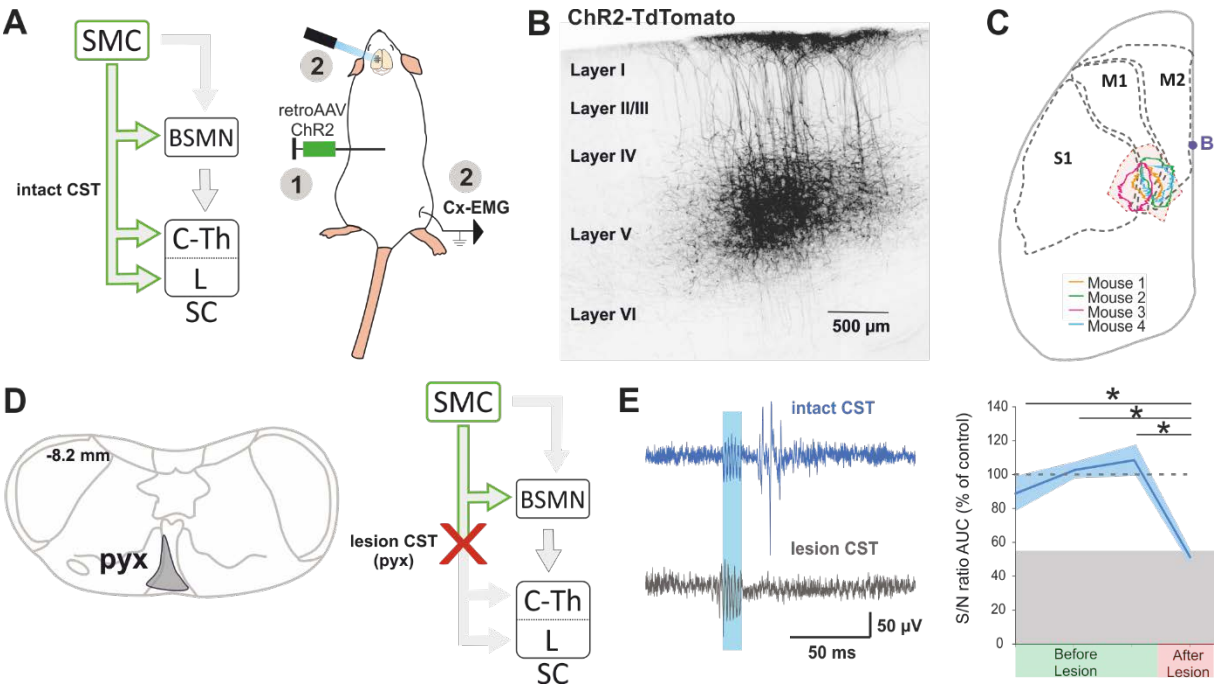

Figure 3. The corticospinal tract can encode muscular contractions.

A. Diagram illustrating corticospinal neurons and their collaterals (*left*), expressing ChR2 after retrograde infection in the lumbar cord with a retroAAV (*right*). The photostimulation and EMG recording session took place at least 3 weeks after the infection.
B. Sagittal image from the sensorimotor cortex (Lateral= 0.68 mm), showing retrogradely labeled corticospinal neurons (expressing ChR2-TdTomato fluorescence).
C. Labeled corticospinal neurons in the 4 animals (colored lines) are within the area functionally determined as inducing DRPs and EMGs in the hindpaw (dashed lines).
D. *Left*, Anatomical extent of the pyramidal lesion in the animal whose recordings are illustrated in I. *Right*, diagram showing the supraspinal collaterals of ChR2-expressing CS neurons spared by the pyramidotomy.
E. *Left*, cortically evoked EMG recordings before (blue) and after (grey) the pyramidal lesion. *Right,* the pyramidotomy abolishes cortically-evoked EMG ($p=0.013$, one-way ANOVA, n= 3 mice). Post-hoc test Holm-Sidak, $^*P < 0.05$. Grey zone: noise level (see Methods)

The blue window on recording traces indicates light stimulation. SMC: sensorimotor cortex, BSMN: brain stem motor nuclei, C-Th: cervico-thoracic spinal cord, L-SC: Lumbo-sacral spinal cord.

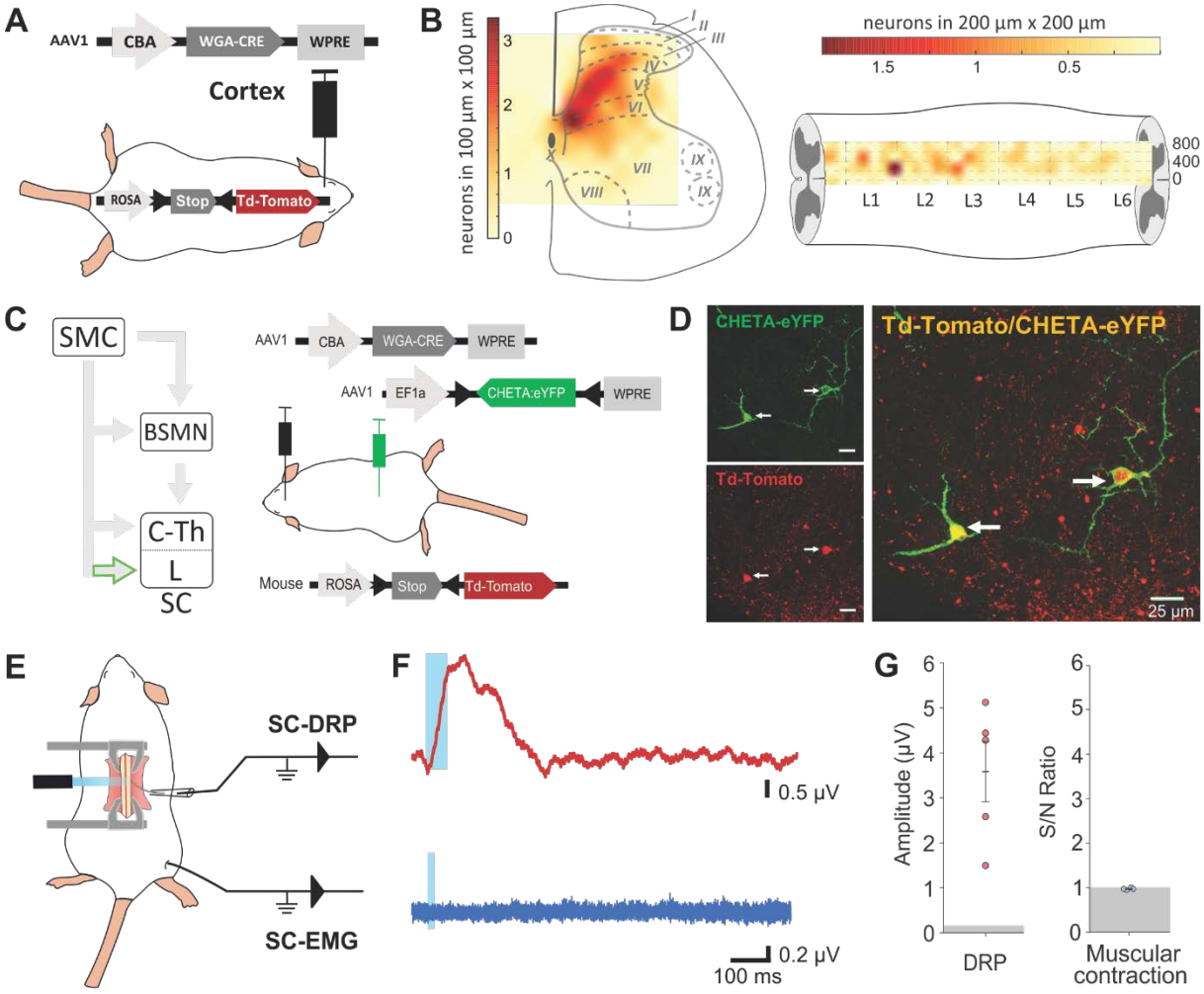

Figure 4. Lumbar corticospinal postsynaptic neurons encode DRPs but no movements.

A. Labeling of CSPNs through a transynaptic approach consisting of AAV1-CBA-WGA-CRE injection in the cortex of TdTomato-flex mice.
B. Localization of CSPNs: heatmap showing the distribution of the neurons in the lumbar cord (6 mm long) projected into the transverse plane (average of 9 mice) (*left*) or horizontal plane (average of 6 mice) (*right*) plane.
C. *Left*, Diagram illustrating that only lumbar direct targets of the CST express CHETA in the following experiment. *Right*, Scheme of the experimental approach consisting in injection of AAV1-CBA-WGA-CRE in the hindlimb sensorimotor cortex and AAV1-Efl-flex-CHETA-eYFP in the L4 spinal segment of a TdTomato-flex mice.
D. Images of CSPNs in the dorsal horn of the spinal cord (laminae V/VI); the arrows point at two CSPN TdTomato+ that express CHETA-eYFP.
E. Schematic experimental design illustrating spinal photostimulation of lumbar CSPNs.
F. Representative traces of DRP (red trace, average of 30 traces) and EMG (blue trace, average of 3 traces) recording from the same animal after CSPN photostimulation (blue window).
G. Photostimulation of lumbar CSPNs induces DRPs (left) but no EMG signal (right). Grey zone: noise level (see Methods).
A. SMC: sensorimotor cortex, BSMN: brain stem motor nuclei, C-Th: cervico-thoracic spinal cord, L-SC:Lumbo-sacral spinal cord.